The 2014 World Congress on
Advances in Civil, Environmental, and Materials Research (ACEM14)
Busan, Korea, August 24-28, 2014

State-of-the-Art Knowledge about Behaviour of Transmission Line Structures under Downbursts and Tornadoes

Ashraf El Damatty[1)*], Amal Elawady[2)], Ahmed Hamada[3)], and William E. Lin[4)]

[1), 2), 3)] *Civil and Environmental Engineering, Western University, London, ON, Canada*
[4)] *Mechanical and Materials Engineering, Western University, London, ON, Canada*
[1)] *damatty@uwo.ca*

ABSTRACT

The ubiquity and full integration of electronics into modern life means that power outages due to Transmission Line (TL) failure are unacceptable from the standpoint of both social and economic losses. HIW events (downbursts and tornadoes) are believed to be responsible for more than 80% of all weather-related transmission line failures worldwide. Previous meteorological and wind engineering studies reported that the wind events in thunderstorms fundamentally differ from the conventional boundary layer wind. Prominent differences are seen in the vertical profile of wind velocity and the localized nature of thunderstorm events. Motivated by the failure of a number of transmission line support towers in Canada, an extensive research program was initiated at the University of Western Ontario (UWO) a decade ago and is still progressing with the aim of developing knowledge and information for designing transmission line structures to sustain HIW events. This paper presents a detailed summary of the literature review and state-of-the-art knowledge on the response of TL systems under HIW events. The paper provides a review of the wind field characteristics of both tornado and downburst events. The review includes field measurements in addition to various numerical methods to simulate these events. The study also presents different attempts at structural modeling and prediction of the behaviour of TLs under HIW events. The first section of this study covers downburst studies while the second section covers tornado studies. Critical load cases obtained from the research conducted at UWO are introduced. At the end of this study, a list of the main findings and recommendations for future research are provided.

Keywords: Dynamic response, Transmission Line, Conductors, Non-Synoptic Winds, Downburst, Tornado, Gust Factor.

1. **INTRODUCTION**

Electricity is carried by Transmission Lines (TLs) from the source of power generation to the distribution system. Overhead transmission lines consist mainly of support towers, conductors, insulators and ground wires. Conductors are responsible for transmitting the electricity and they are attached at insulators to the towers. Ground wires protect the line from lightning strike. Optimal TL design is particularly important when the site of power generation is geographically remote from population centers, such as in the case of many hydroelectric dams in North America. Past reports of TL failure due to weather conditions (Dempsey and White, 1996; Li, 2000), including High Intensity Wind (HIW) events (downbursts and tornadoes), emphasize the importance of accurate design wind loads. The current review summarizes the previously conducted work related to the behaviour of TL under non-synoptic winds in order to identify the limitations and gaps in current codes and to suggest how these gaps can be closed. This paper consists of three main sections. The first section covers the response of TL structures under downburst winds. This section provides a description of the downburst wind field and a literature review showing previous field measurements and numerical modeling of downbursts. Section two focuses on the response of TL structures under tornado wind fields. This section provides a description of the tornado wind field and a literature review for structural modeling of transmission line structures under tornado loading. The third section provides the main findings and recommendations for both downburst and tornado loading.

2. RESPONSE OF TRANSMISSION LINES TO DOWNBURST WINDS

2.1. Description of downburst wind field

A downburst is defined as an intensive downdraft of air that induces very strong wind in all directions when striking the ground. Fujita (1985) defined a downburst as a mass of cold and moist air that drops suddenly from the thunderstorm cloud base, impinges on the ground surface, and then horizontally diverges from the centre of impact as shown in Fig. 1. In basic terms, downbursts are downdrafts with sufficient energy to reach ground level.

Fig. 1 Downburst event [source: http:// malumnalu.blogspot.ca/2009/12/hurricane-katrina-incredible-pictures.html]

2.2. Field measurements and numerical modeling of downbursts

(A) Field measurements during downbursts

Wind field prediction for downbursts is a major challenge because of their localized nature. A limited number of field measurements for downbursts are available in the literature. These include the Northern Illinois Meteorological Research (NIMROD) and the Joint Airport Weather Studies (JAWS) reported by Fujita (1990), and the FAA/Lincoln Laboratory Operational Weather Studies (FLOWS) reported by Wolfson *et al*. (1985). The initial diameter (D_J) of the downdraft reportedly ranges between 600 and 1700 m as provided by Hjelmfelt (1988). The variable nature of downbursts, both spatially and in time, makes full-scale study a difficult task.

(B) Downburst numerical modeling

Due to the difficulty of field measurements for downbursts, most of the research has relied on numerical modeling or reduced-scale physical modeling (i.e. experiments) to predict the downburst wind field as well as the response of structures to such events. Three numerical approaches are available in the literature and can be summarized as follows: a) Ring Vortex Model, b) Impinging Jet (Impulsive Jet) Model, and c) Cooling Source (Buoyancy-Driven) Model, and these are shown in Fig. 2. The Ring Vortex Model (Zhu and Etkin, 1985; Ivan, 1986; Vicroy, 1992; Savory *et al*., 2001) simulates the vortex ring that is formed during the descent of the downdraft air column. As reported by Savory *et al*. (2001), the Ring Vortex Model is not accurate in simulating the downburst field near the ground after the air column touches the ground.

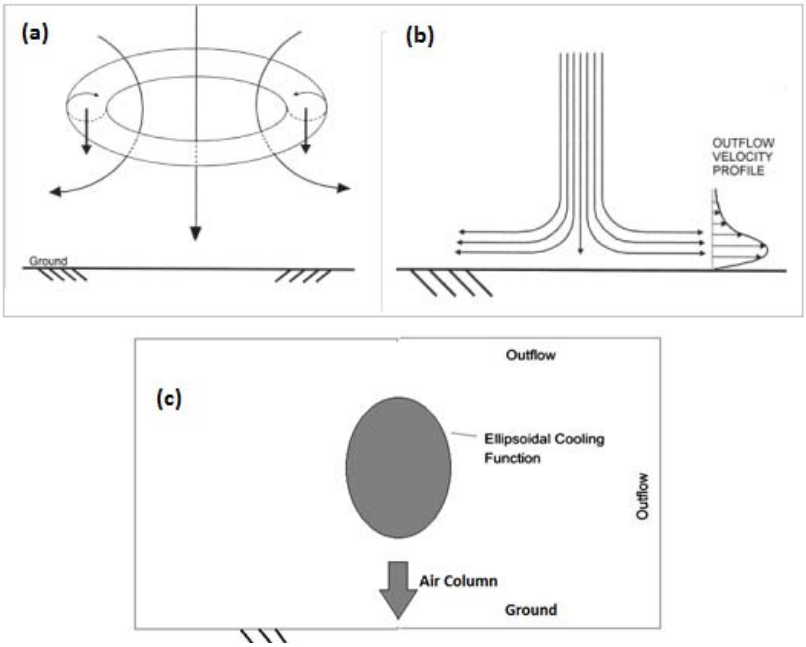

Fig. 2 a) Vortex Ring Model, b) Impinging Jet Model and c) Cooling Source Model (diagrams are from Savory *et al.* (2001b) and modified from Vermeire *et al.* 2011)

The impinging jet model is based on the analogy between an impulsive jet impinging upon a flat surface and a downburst (Fujita, 1985). The cooling source method is based on introducing a cooling source inside the computational domain simulating the cooling process in the cloud base. This cooling process increases the weight of the cloud base and initiates the downdraft. Selvam and Holmes (1992) developed a two-dimensional, steady numerical model for an impinging jet. Hangan *et al.* (2003) improved this basic Computational Fluid Dynamics (CFD) model and validated their CFD assumptions by carrying out pressure and velocity measurements with an impinging jet. Kim and Hangan (2007) compared their simulated mean wind profile with full-scale data (Wood *et al*., 2001), experimental results (Didden and Ho, 1985; Donaldson and Snedeker, 1971), as well as a generic 1/7 power law boundary layer profile. These CFD models of an impinging jet yielded time series for a vertical (axial) component (V_{VR}) of the velocity field, as well as a horizontal (radial) component (V_{RD}). At a fixed point in space, these two velocity components are functions of horizontal location relative to the centre of the jet and height relative to the ground. Fig. 3 illustrates the spatial variables for an impinging jet model in plan view. These variables are the jet diameter (D_J), and the location of the downburst centre relative to the tower (represented by the polar coordinates R and Θ).

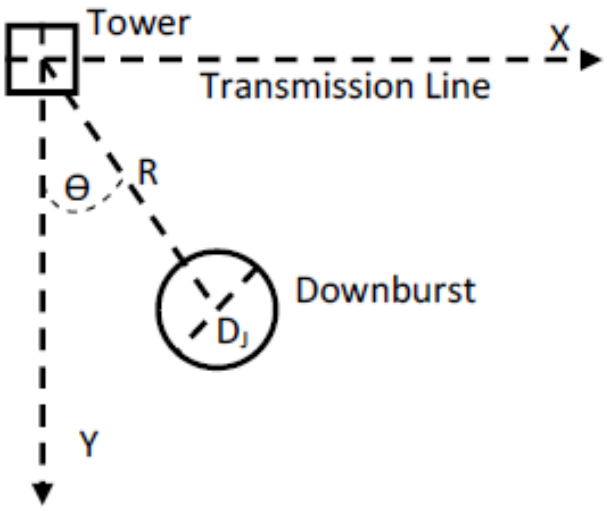

Fig. 3 Downburst parameters with respect to the tower of interest

Shehata *et al.* (2005) conducted an extensive parametric study to investigate the downburst wind profiles. Fig. 4 illustrates the variation of the radial velocity, normalized with respect to the initial jet velocity, along the height. The maximum velocity profile was found to occur at an R/D_J value of 1.2. The absolute maximum velocity is approximately equal to 1.1 V_J. El Damatty *et al.* (2013) reported that the value 1.1 V_J can be considered as a design reference velocity at 10 m height (V_{10}). However, it should be emphasized here that, at any instant, the resultant wind speed may have a

vertical component in addition to a horizontal component as shown in Fig. 5. Mara *et al.* (2010) found that the wind inclination can reach 20° above horizontal in a critical case for a lattice tower. Fig. 6 shows the variation of the reference velocity, V_{10}, normalized with the jet velocity, V_J, for different values of jet diameter. This figure indicates that the absolute maximum velocity, which occurs at R/D_J of 1.2, increases with decreased jet diameter. Furthermore, for the time variation, the time history of the radial velocity component (V_{RD}), as well as the vertical velocity component (V_{VR}), follows a trend with a maximum peak followed by a minimum peak as shown in Figs. 7 and 8. The subsequent stabilization at a constant value is an artifact of a simulation approach in which the jet momentum source starts impulsively (correct) but then is left on (non-physical). After the peak, wind speed decays to the local environmental wind speed associated with the storm translation when the thermo-fluidic forcing, by the cold and dense initial parcel at cloud level, is exhausted. In the parametric study conducted by El Damatty *et al.* (2013), the time of occurrence of the maximum radial velocity was found to be proportional to the factor (D_J/V_J).

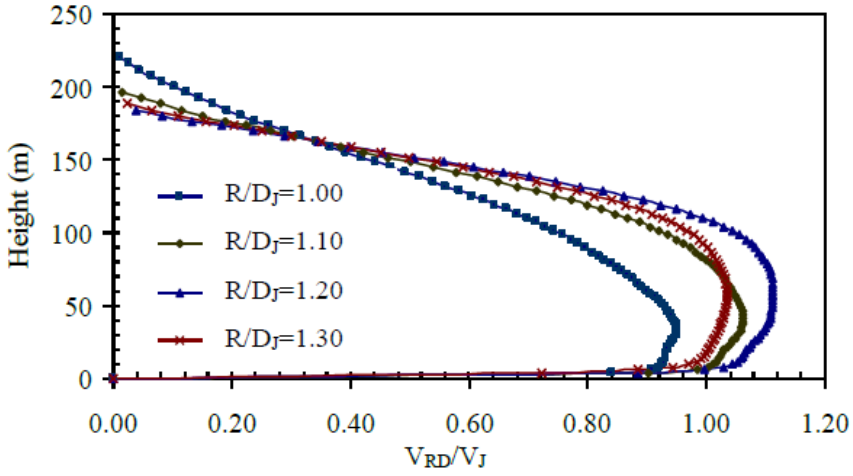

Fig. 4 Vertical profile of the horizontal/radial outflow wind speed (Shehata *et al.,* 2005)

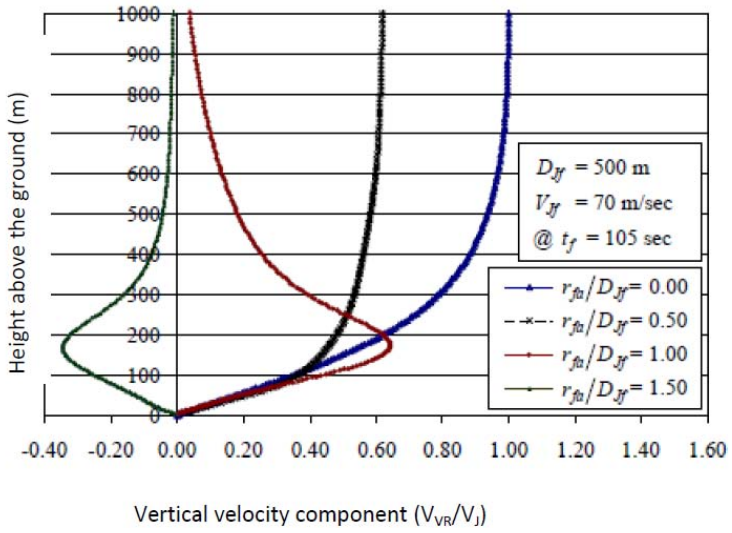

Fig. 5 Vertical profile of the vertical/axial outflow wind speed (Shehata *et al.,* 2005)

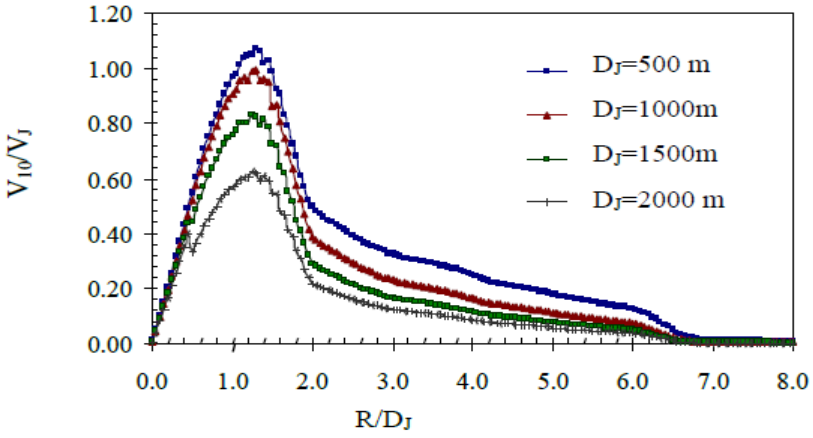

Fig. 6 Downburst reference horizontal velocity (V_{10}) at 10 m height. (Shehata *et al.,* 2005)

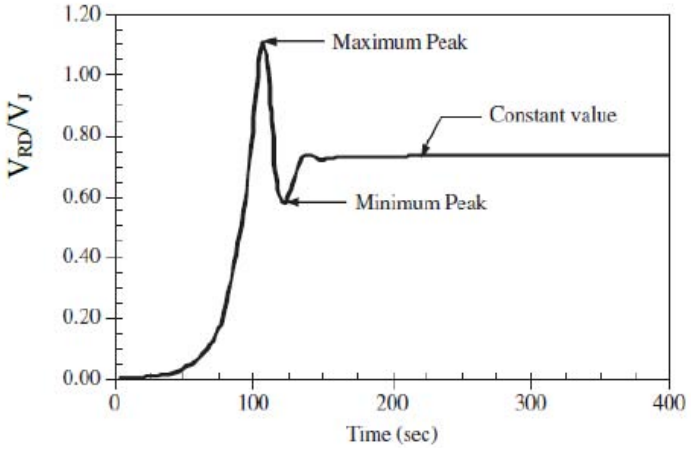

Fig. 7 Typical time history of the horizontal/radial velocity (Shehata and El Damatty, 2007)

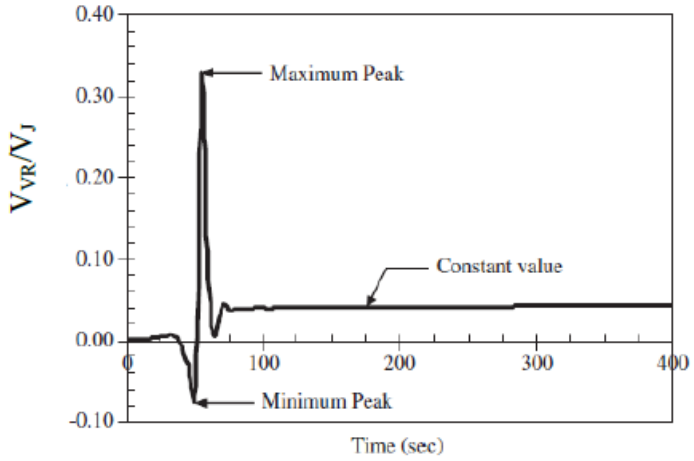

Fig. 8 Typical time history of the vertical/axial velocity (Shehata and El Damatty, 2007)

Sengupta and Sarkar (2008) simulated downbursts using the impinging jet method employing k-epsilon, k-omega, Shear Stress Transport (SST) turbulence models, as well as Large Eddy Simulation (LES), and compared the resulting profiles with those from an experiment. Their results showed a reasonable agreement between the profiles obtained from the LES and from the experiment. The applicability of using LES to simulate downbursts is also indicated from the results of Hadžiabdić (2005), Chay *et al.* (2006) and Gant (2009).

Mason *et al.* (2009) implemented the cooling source method based on a dry, non-hydrostatic, sub-cloud and axisymmetric model. One year later, Mason *et al.* (2010) extended this work to a three-dimensional model. Both studies used the Scale Adaptive

Simulation (SAS) method developed by Menter and Egorov (2010), which is an improvement for the unsteady Reynolds-Averaged Navier–Stokes (URANS) method used to predict unsteady turbulent flow. However, Gant (2009) reported that the SAS method appeared to over-predict the turbulent viscosity of jet-type flows. Vermeire *et al*. (2011a) simulated downbursts using the cooling source approach with Large Eddy Simulation (LES) and the results showed good agreement with Mason *et al*. (2009) and disagreement with impinging jet models.

Most studies have considered a single downburst column whereas in a study that modeled two downbursts, representing part of a downburst line commonly occurs in nature, Vermeire *et al.* (2011b) showed that two adjacent downbursts may result in peak near-ground wind speeds that are 55% greater than those associated with one of those downbursts on its own, together with a 70% greater damage footprint. However, even cooling source models neglect some of the other key physics of real events, notably the forcing is associated with precipitation, and the fact that such events are not truly axi-symmetric. Recently, LES simulation of a complete downburst-producing thunderstorm (Orf *et al.,* 2012) has revealed the complexity of downburst outflows, although circumferential averaging of the wind field suggests that it may be possible to estimate the highest wind speeds at any time within the event by using the averaged wind field (essentially an axi-symmetric metric) multiplied by a consistent peak factor (Orf *et al.*, 2013).

Design codes define the wind speed at any point as being the sum of a mean wind component (non-turbulent) and a turbulent component. Most studies have considered only the non-turbulent component of downburst wind velocity. The turbulence characteristics are essential for quantifying the peak loads and responses experienced by surface structures as indicated by Kwon and Kareem (2009), Chen and Letchford (2004a; 2004b), Chay *et al*. (2006; 2008) and Holmes *et al*. (2008). Recent downburst simulations have considered the effects of terrain roughness (Mason *et al*., 2009; 2010a; Vermeire *et al*., 2011a) and topography (Mason *et al*., 2010b) on downburst and synoptic winds. Terrain roughness in these studies was modeled using neutral wall functions. Wall functions are typically used to simulate the wall bounded flow using an economical number of computational grid layers. Without using a wall function, simulation of wall bounded flows such as downbursts, requires a large number of grid layers near the ground to correctly capture the steep velocity gradient. Terrain roughness is typically characterized by the aerodynamic roughness length, z_0, summarized in Table 1 for different types of terrain. According to Blocken *et al*. (2007), the maximum roughness z_0 that can be accurately modeled by a wall function is governed by $\Delta_z > 60\ z_0$, where Δ_z is the height of the first computational grid layer above the wall. Mason *et al*. (2009) and Vermeire *et al*. (2011a) used Δ_z equal to 1.0 m with the implication that their results are valid for aerodynamic roughness length of less than 0.016 m, i.e. smoother than standard open terrain.

Table 1 Aerodynamic roughness length for wind over various terrains (Wieringa 1992)

Terrain exposure	z_0 (m)
Smooth	0.005
Open	0.03
Roughly open (suburban)	0.25
Very rough (forest or urban)	1.00

The aforementioned studies of downburst wind loads provided a good base of knowledge about mean flow characteristics. However, the characteristics of the turbulence (e.g. turbulence intensities or length scales) associated with downbursts are yet to be fully clarified. Fig. 9 gives an indication of the contribution of the turbulent component to the overall downburst wind velocity. An envelope of the peak response can be approximated by scaling up the mean component alone. Most quasi-static analyses of TLs have relied on this scaled mean approach.

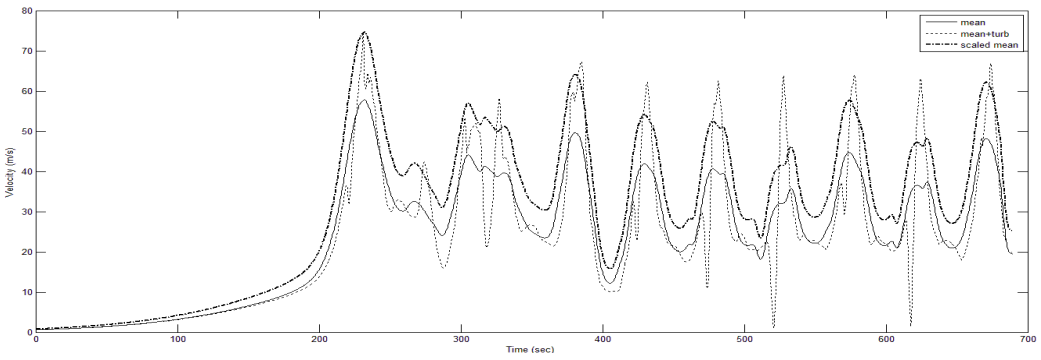

Fig. 9: Contribution of the turbulent component to the overall wind velocity

Turbulence intensity quantifies the magnitude of wind velocity fluctuations relative to a mean wind velocity. Turbulence length scales give indications of the size of the flow structures that affect the span reduction factor and the gust factor (Holmes *et al*., 2008). The turbulence associated with downbursts plays an important role when quantifying loading for the design of transmission lines. For the case of synoptic wind loading, design codes (ASCE 74 2010; AS/NZS:7000, 2010) apply a gust load factor to account for the reduction of the turbulence correlation with space, the terrain type and the dynamic response of the structure. In case of typical transmission lines with support

tower heights of 50 m or less, dynamic response is usually neglected due to the high aerodynamic damping of the conductors and the high natural frequency of the tower. Treating a downburst outflow as a gust front, Kwon and Kareem (2009) presented an alternative analysis framework called the gust-front factor approach, which is similar to the gust load factor for synoptic wind, whereby a factor was proposed for scaling up conventional wind loads so as to match the loads resulting from gust-front winds. This approach contains various components affecting the loading due to gust-front winds, such as a kinematic effects factor for the variation in the vertical profile of wind speed, a pulse dynamic factor for the dynamic effects introduced by the sudden rise in wind speed, a structural dynamics factor for the non-stationarity of turbulence in gust-front winds and a potential load modification factor to represent the transient aerodynamics.

2.3. Structural modeling of a transmission line under downburst loading

2.3.1 Lattice tower and guy wires

Shehata *et al*. (2005) developed a finite element model to simulate the tower members and the guy wires as a two-node, linear, three-dimensional frame element with three translational and three rotational degrees of freedom per node. Each tower member was simulated by one element while each guy wire was modeled by five elements. Rigid connections were assumed between the tower members as these are physically connected using multi-bolted connections that can transfer moments. The conductors were studied separately and then their reactions were reversed and applied at the tower connection points. For the downburst loading, a procedure was developed to scale up a small impinging jet wind field (Hangan *et al.*, 2003). Shehata and El Damatty (2007), Shehata and El Damatty (2008), and Shehata *et al*. (2008), studied a guyed tower while Darwish and El Damatty (2011) studied the behaviour and the failure modes of a self-supported tower. El Damatty and Aboshosha (2012) studied both guyed and self-supported towers to assess the behaviour and the failure modes. Ladubec *et al*. (2012) improved upon the linear analysis by Shehata and El Damatty (2008) and studied the P- effect in tower response to a downburst wind field by using nonlinear space frame elements to simulate the tower members. The study showed an increase of 20% in the peak axial forces in the chord members of the main legs, as compared to the results from a linear analysis.

The inclusion of the turbulent component in the structural analysis may magnify the response, due to the combined effects of the fluctuating (background) component and the resonant component, which means a lower failure capacity. Wang *et al.* (2009) studied the dynamic effect of a downburst on tall transmission towers. Wind tunnel tests were conducted to determine the wind load coefficients of the transmission towers and then the towers were analyzed under downburst wind loading. Dynamic effects were minor due to the relatively high natural frequency of the towers compared to the natural frequency of the wind event.

Lin et *al.* (2012) developed an aeroelastic model for a single span of a transmission line. The guyed lattice tower was simplified to an equivalent mast at a length scale of 1:100 while synoptic or downburst wind loading were applied with a time scale of 1:10. In either case of atmospheric boundary layer or downburst wind loading, the structural response was generally quasi-static. Resonant dynamic response was less evident with the downburst wind than with the synoptic wind.

2.3.2. Conductor lines

Finite Element Analysis (FEA) with the 2-D non-linear consistent beam element (Koziey and Mirza, 1994) has been modified by Gerges and El Damatty (2002) to include the geometrical non linear effects, and was utilized by Shehata *et al*. (2005) to accurately simulate conductor line properties and predict reactions for downburst loading. Fig. 10 shows an element and each cable span is modeled as ten elements. They considered the geometric non-linearity due to large line span and relatively small line cross-section, which causes large displacements from wind loading, as was modeled by Desai *et al*. (1995) with a three-node iso-parametric finite element. The analysis was performed in the horizontal and the vertical directions separately to obtain the response under the radial and vertical downburst velocities, respectively. The 2-D element was acceptable for downbursts as their associated velocities in the horizontal direction are much higher than those in the vertical direction and, thus, decoupling between the two directions can be justified. Shehata *et al*. (2005) reported that modeling six conductor spans, as shown in Fig. 11, is enough to obtain accurate results of the transmitted forces from the conductor to an intermediate tower.

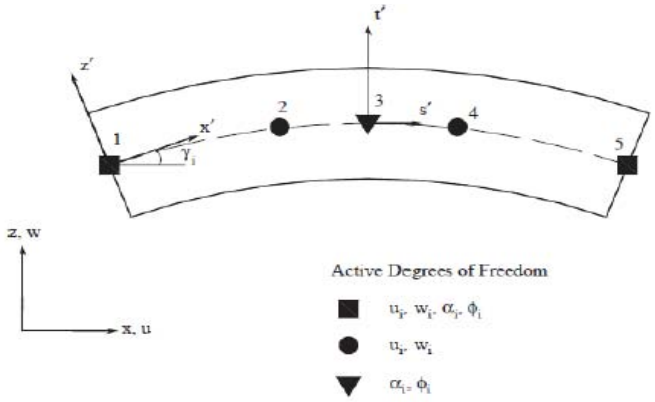

Fig. 10 Consistent beam element coordinate systems and degrees of freedom (Gerges and El-Damatty, 2002)

Fig. 11 Modeling of the transmission line under study (Shehata *et al.*, 2005)

Savory *et al*. (2001) studied the failure of transmission towers in the cases of tornado and downburst wind loading. Conductor forces were neglected and, as a result, failures were only associated with tornado loading and no failure was observed with downburst

loading. On the contrary, Shehata *et al*. (2005) predicted three different failure modes for transmission towers with downbursts. This is mainly due to the strong effect of a downburst upon a relatively localized region of a transmission line. The most critical failure mode was found to be due to the significant variation in the longitudinal tensile forces from the lines upon the support towers. Shehata *et al*. (2005) revealed that this is the most critical failure mode as the resultant, large, longitudinal force transmitted to the tower cross-arms leads to an out-of-plane bending moment in this region. El Damatty and Aboshosha (2012) discussed a similar mode of failure. Aboshosha and El Damatty (2013a) conducted a parametric study to check the expected values of the conductor longitudinal forces. With a jet velocity of 40 m/s, the longitudinal force transmitted to the tower due to the unbalanced tension was up to 60% of the transverse force.

El Damatty *et al.* (2013) showed that since the conductor structural response is highly nonlinear, different conductor types would experience different responses based on the conductor characteristics. They concluded that the main parameters that affect the longitudinal and transverse forces on a conductor are its material, cross-sectional area, projected area, span, insulator length and sag. The inclusion of the flexibility of the insulators at tower/conductor connections, rather than assuming fully-hinged boundary conditions, also has a significant effect on the natural frequencies and mode shapes. Line sag is inversely proportional to the pre-tensioning force. The level of the pre-tensioning force is found to have a major influence upon the natural periods and mode shapes of line vibrations due to the effect of sag on the conductor's stiffness (Darwish *et al.*, 2010). In addition, environmental factors such as temperature, highly affect the conductor sag where the actual sag at the time of downburst occurrence may vary from reported values. High flexibility and the expected nonlinear behaviour of the conductors result in a time consuming FEA procedure, since many iterations are required to investigate different downburst configurations that lead to the critical case of loading (Aboshosha and El Damatty, 2013b). In view of this fact, there is a need for a computationally efficient technique that can analyze multi-span conductors under both vertical and horizontal HIW loading and can take into consideration the conductor properties.

Irvine (1981) derived a closed-form solution for the reactions of a single-spanned conductor, where the loading can be fitted with a third-degree polynomial. In addition, Yu *et al*. (1995) considered highly concentrated loads to derive an exact solution to calculate the reactions for a single conductor span. Both solutions neglected the flexibility of the insulators, which Darwish *et al*. (2010) concluded was important in quantifying the forces carried by the towers. Although Winkelman's earlier solution (1959) accounted for the insulator flexibility, the differences between tensile forces on conductors in adjacent spans was neglected and, as such, the longitudinal reactions that are transmitted from the conductors to the supporting towers would be ignored. Based on the analytical solution for an elastic catenary, Ahmadi-Kashani and Bell (1988) and Wei *et al*. (1999) developed cable elements to simulate a whole span. Although this solution is more efficient, due to the reduction in degrees of freedom, these elements were only developed for uniform wind load and are not suitable for HIW. Subsequently, Aboshosha and El Damatty (2013b) developed a numerical technique to analyze multi-spanned conductors under HIW. This solution is the first semi-closed

form solution for a multi-spanned conductor system under non-uniform loading in both the vertical and horizontal directions, where insulator rigidity is considered. The technique was approximately 185 times faster than FEA.

Darwish *et al*. (2010) modified the two-dimensional nonlinear finite element model of the transmission lines developed by Shehata *et al*. (2005) to study the dynamic characteristics of the conductors under turbulent downburst loading. The turbulence component was extracted from full-scale data and then added to the mean component of the downburst wind field developed by Kim and Hangan (2007). Large deformations and the pre-tension loading were modeled. The aerodynamic damping was determined with an expression given by Davenport (1967), which was derived for synoptic winds and assumed an average velocity in the calculation of the aerodynamic damping in order to overcome the localized nature of downbursts as the wind velocity varies with time and also spatially along the conductor length. The study concluded that the resonant component due to the turbulence is negligible due to the large aerodynamic damping, the dynamic response is mainly due to the background component of wind velocity fluctuations and turbulence accounted for almost 20% of the conductor deflection and reactions. In addition, the study discussed the effect of pre-tension force on the natural period and mode shapes of the conductors.

Holmes *et al*. (2008) isolated the turbulent component of the downburst velocity and produced a peak load reduction factor for the spatial variation along the longitudinal direction from a set of impinging jet CFD data (Kim *et al*., 2007). The span reduction factor (SRF) was found to range between 1 and 0.8 for a separation of 720 m with downburst wind loading. A similar result was found for the vertical velocity profiles. The effect of terrain roughness and height on SRF remains uncertain.

2.3.3. Critical configurations of a downburst on a transmission line

Shehata *et* al. (2005), Shehata and El Damatty (2007), Shehata *et al*. (2008) and Darwish and El Damatty (2011) adopted quasi-static analysis procedures (relevant for a mean component that varies slowly with time) with the downburst wind field from Hangan and Kim (2007) as an input. Shehata *et al.* (2005) reported that the effective period for downburst wind speed variation ranged between 20 and 22 seconds while the vibration frequencies for the transmission tower and conductor were 0.58 sec and 8.25 seconds, respectively. As such, no strong dynamic effect was evident.

Using the structural analysis model developed by Shehata *et al*. (2005), Shehata and El Damatty (2007) conducted a parametric study to investigate the critical downburst configuration by varying the jet diameter (D_J) and the location of the downburst centre relative to the tower (R). A guyed transmission tower, which collapsed in Manitoba in 1996 due to a downburst event, was used to perform this parametric study. The critical downburst parameters, in terms of the size of the event and its location relative to the tower, leading to maximum forces in the tower members, were identified. The study revealed that the critical downburst parameters vary based on the type and location of the members. Unsurprisingly, the chord members, diagonal members and cross-arm members were susceptible to different critical downburst configurations. Shehata and El Damatty (2008) extended their numerical scheme by including a failure model for the tower members, which was used to study the progressive collapse of the tower failure. An optimization routine was implemented by Shehata *et al*. (2008) to predict the critical downburst parameters and the

corresponding forces on a transmission line by an automated procedure. This finite element-optimization technique was validated by comparing the maximum forces and critical downburst parameters in a number of tower members to the corresponding values obtained from an extensive parametric study. The study showed that the most critical members are at the cross-arms supporting the guy wires and conductors. In addition, Shehata *et al.* (2008) reported that wind loads have a minor effect on the internal forces within members located below the guy attachment height on the tower. For cross-arm members, the internal forces result mainly from the wind loads acting on the conductors, though. Fig. 12 shows a failure of cross-arms documented by an electric energy provider.

Fig. 12 Field evidence of lattice tower failure at cross-arms (Manitoba Hydro, 1999)

Darwish *et al.* (2010) investigated the importance of the translation velocity of the downburst, using three critical downburst configurations. It was found that the tower failed at the same radial velocity regardless of the contribution of the translational component to this velocity. Therefore, Darwish *et al.* (2010) reported that there is no need to consider the translation velocity of the downburst and it is sufficient to vary the location of the downburst in space for a large number of separate stationary events. In addition, Darwish *et al.* (2010) found almost no variation in the dynamic characteristics of the conductors under the different loading configurations. Darwish and El Damatty (2011), El Damatty and Aboshosha (2012), Aboshosha and El Damatty (2013c) and El Damatty *et al.* (2013) performed additional parametric studies to investigate the critical downburst configurations. The studies agreed that changing the location of the downburst (R/D_J and θ) has a stronger effect on the value of the axial force in all tower members when compared to changing the downburst size (D_J) which has a minor effect. In addition, the ratio of the span (L) to the jet diameter, D_J, plays a vital role in the existence of these critical cases. El Damatty *et al.* (2013) proposed three critical load cases for calculating static forces upon towers and conductors under downburst loading, where the loads should be applied on both the tower of interest as well as the six closest conductor spans. The three cases are shown in Figs. 13 and 14 and explained

below:

(1) At Θ = 0°, R/D_J = 1.20 and D_J = 1000 m, the downburst outflow is modeled as impacting perpendicular to the major axis of the transmission line. The radial velocity applied on the support tower can be considered to be equal to 1.1 V_J. To approximate the conductor's transverse reaction, an equivalent uniform velocity distribution with a magnitude of 0.92 V_J can be used, as shown in Fig. 13b.

(2) At Θ = 90°, R/D_J = 1.20 and D_J = 1000 m, the same wind load profile is applied on the tower face parallel to the major axis of the line, as in the previous case, while no wind load is applied on the conductors.

(3) At Θ = 30°, R/D_J = 1.60 and D_J = 500 m, the vertical profiles of velocity in the direction perpendicular and parallel to the line can be approximated as having uniform values of 0.75 V_J and 0.43 V_J, respectively, to stipulate the tower wind load. A difference in downburst radial velocity distribution at the two adjacent conductors results in a nonlinear longitudinal force acting on the tower. Design charts for the wind loading on conductors were given.

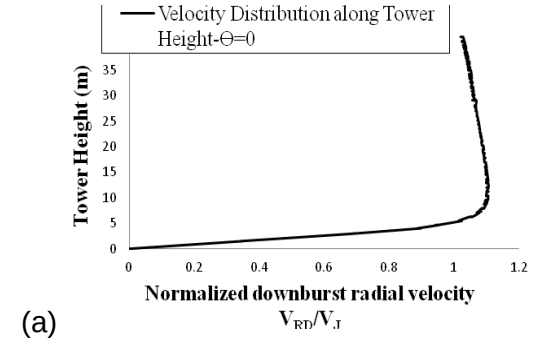

(a)

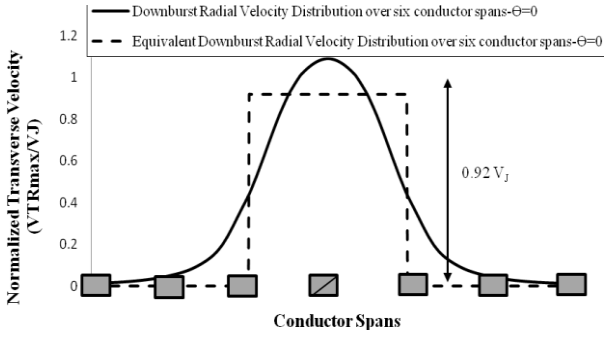

(b)

Fig. 13 (a) V_{RD} distribution along tower height with = 90° and 0°, R/D_J = 1.2 and D_J = 1000 m and (b) V_{RD} distribution over six line spans with = 0°, R/D_J = 1.2 and D_J = 1000 m (El Damatty *et al.*, 2013)

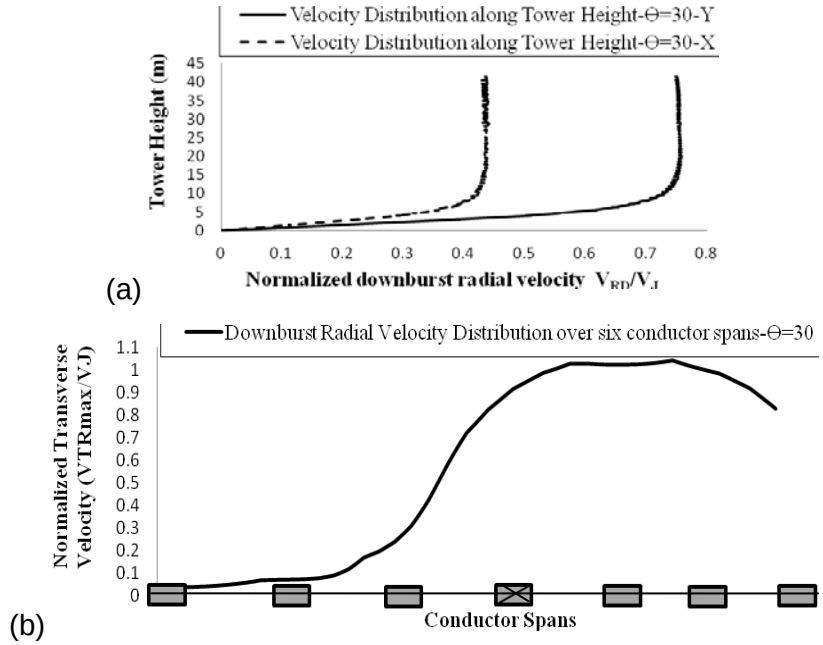

Fig. 14 (a) V_{RD} distribution along tower height with = 30°, R/D_J = 1.6 and D_J = 500 m and (b) V_{RD} distribution over six line spans with = 30°, R/D_J = 1.6 and D_J = 500 m (El Damatty *et al.*, 2013)

3. RESPONSE OF TRANSMISSION LINES TO TORNADO WIND FIELDS

3.1 Tornado wind field

In Canada, tornadoes occur in the southern regions of Alberta, Manitoba, Saskatchewan, Ontario and Quebec. Ishac and White (1994) reported that, for populated areas in Canada, southwestern Ontario experiences the highest rate of tornado incidence (about two tornadoes per 10,000 km^2 every year and most transmission line failures in this area are caused by tornadoes. 92% of these tornadoes were F2 or less on the Fujita scale. Ontario Hydro has reported that five out of six weather related line failures in their territory are due to tornadoes (Behncke and White, 2006). Newark (1984) concluded that, on average, a F3 tornado occurs in southwestern Ontario every five years. In the United States, 800 to 1,000 high-intensity wind storms occur each year leading to damage or failures of transmission structures (Behncke and White, 2006). The CIGRÉ (2001) questionnaire on line failures indicated that 65% of weather-related events on transmission lines were caused by tornadoes. Despite these facts, the codes of practice, design guidelines and utilities design methodologies are based on the loads resulting from large-scale synoptic events, which generate conventional boundary layer wind profiles. It is well-known from meteorological and wind engineering studies (Holmes and Oliver, 2000; Letchford *et al*., 2002) that the wind events in thunderstorms fundamentally differ from the conventional boundary layer wind. A prominent difference is in the vertical profile of velocity. Conventional wind profiles are characterized by a monotonic increase in velocity with increasing height above ground. However, the velocity profiles for both tornadoes and downbursts have a

maximum near the ground. Another major difference between the gust-fronts generated in HIW events and synoptic winds is that the mean wind speed, as well as the wind direction in some cases, exhibits sharp changes. For the turbulence component, Kareem (2010) concluded that the effects of mechanically-generated turbulence are often much less than the effects of convectively-generated turbulence because these transient HIW events may not have sufficient time to evolve into a well-developed flow that is indicative of the terrain characteristics.

Tornadoes are rotating wind vortices with high wind speeds affecting relatively narrow paths as defined by Fujita (1981). They originate from convective clouds that generate rotating columns of air (Twisdale, 1982). The Fujita scale (Fujita and Pearson, 1973) is currently the most widely used measure of tornado effects. It categorizes tornadoes between F0 to F5 based on maximum wind speed, path length and width, and level of damage to surroundings. In 2001, the Texas Tech University Wind Science and Engineering Research Center recommended an alternative categorization, known as the Enhanced Fujita Scale (McDonald *et al*., 2004; Ramsdell, Jr. and Rishel, 2007). The Enhanced Fujita Scale is based on the highest wind speed estimated in the tornado path, but the damage classification is still based on the criteria recommended by the original Fujita Scale. The Enhanced Fujita Scale is not widely used yet and the intent to implement it in design codes and manuals of practice has been considered as perhaps being premature due to wind speed estimates being based upon design practices specific to the USA (Doswell III *et al*., 2009). The tornado wind speed profile is typically decomposed into tangential, radial, and vertical components. Fig. 15 shows vertical profiles of the tangential velocity component of a F4 tornado at various radial distances from the tornado centre.

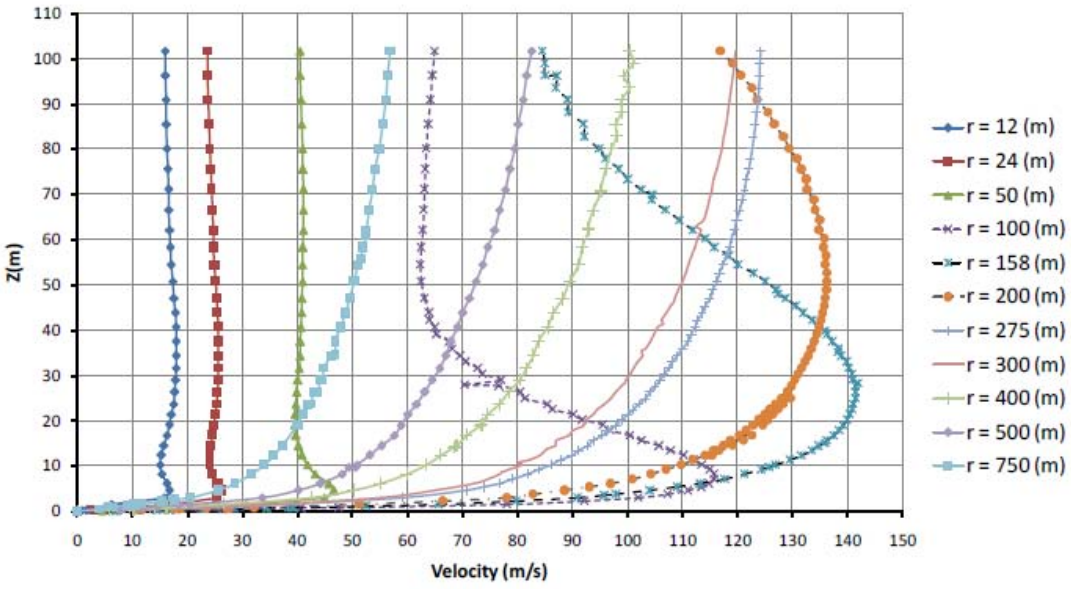

Fig. 15 Vertical profile of tangential component for different radial distances from F4 tornado centre

The size and intensity of tornadoes cannot be measured in the field by traditional recording stations due to the severity and the localized nature of these events. Photographic analysis using videos of moving objects in tornadoes, Doppler radar, and 'post-mortem' damage surveys are typically the only available methods to estimate the tornado wind speeds (McCarthy and Melsness, 1996). Tornado measurement with Doppler radar is not very accurate for the near-ground region. Rare field measurements are available for the 1998 Spencer South Dakota F4 tornado (Wurman, 1998; Sarkar *et al.*, 2005) and the 1999 Mulhall F4 tornado (Lee and Wurman, 2005).

Furthermore, there are some interesting attempts to understand the effects of tornadoes upon structures, based on comparison of a simple analytical wind field model to damage survey observations. Based on the assumption of a circular vortex about a vertical axis, Reynolds (1970; 1977) treated the wind field as a vector sum of the following three wind speed components: rotation about a vertical axis (V_R), linear horizontal translation (V_T) and convergence towards the centre of rotation (V_C). Assuming counter-clockwise rotation (looking down upon the vortex as shown in Fig. 16), it follows that V_R and V_T have a reinforcing effect over the right half of the vortex and a negating effect over the left half (when looking in the direction of translation, which is towards the top of the page for Fig. 16). The resultant wind velocities and pressures at eight cardinal points about the tornado circumference (north, north-east, east et cetera) were determined for ninety combinations of the wind speed components and it was put forth that these could be related to damage patterns. Tipping of the tornado axis and the resulting significant vertical velocities were not considered in this simple model.

Following the development of the Ward-type simulator (Ward, 1972), laboratory experiments have been used to study tornado behaviour near the ground and to describe the characteristics of the tornado-like-vortices phenomena. Tornado simulators were developed over time and led to the creation of the Tornado Vortex Chamber (TVC), which provides a good simulation of the characteristics inside a tornado. However, the boundary conditions have to be carefully applied, as is also true for numerical simulations using CFD software.

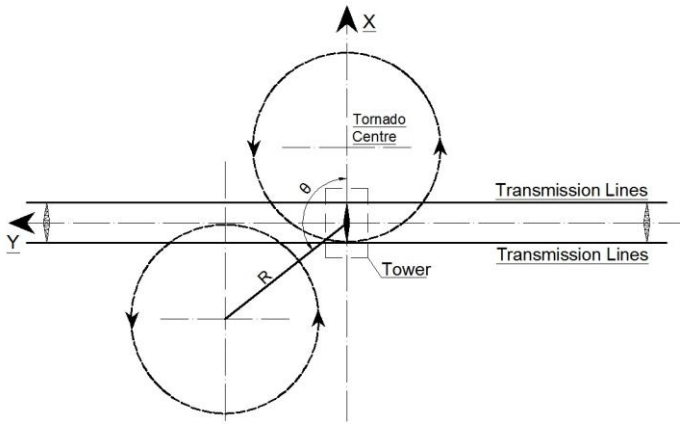

Fig. 16: Tornado configuration relative to a transmission line system

Harlow and Stein (1974) developed one of the first numerical models to simulate

tornado-like vortices. The two-dimensional, axisymmetric model produced both the one-cell and two-cell vortices using a free-slip lower boundary condition. On the other hand, Rotunno (1977; 1979) captured the vortex breakdown of a tornado-like vortex using a no-slip lower boundary condition. The simulations showed the vortex core size to be a function of the swirl ratio. Rotunno (1984) was able to simulate multiple vortices by introducing random noise into a three-dimensional model of a Ward-type TVC. The simulation showed secondary vortices with 20% to 30% greater tangential velocities than the mean flow. Fiedler (1994; 1997) and Trapp and Fiedler (1995) introduced the concept of buoyancy in a rotating cylinder of fluid and used an axisymmetric model to study vortices that formed within a domain with rigid boundaries. It was shown that vortex touchdown produced wind speeds in excess of the thermodynamic speed limit by a factor of 5 and, at higher swirl ratios, produced multiple vortices. Lewellen *et al*. (1997) and Lewellen *et al*. (2000) modeled full-scale tornado flow using LES simulations and their analysis of the flow dynamics showed the influence of turbulence in generating high wind speeds near the ground and the production of multiple vortices at high swirl ratios. Hangan and Kim (2008) conducted a simulation using a commercial CFD program (FLUENT Inc., 2005). Their simulation with a swirl ratio of S = 0.28 was validated by a comparison with Baker's experimental results (1981) from a Ward-type vortex chamber. The numerical simulation was then extended by considering S = 0.10, 0.4, 0.7, 0.8, 1.0 and 2.0. The resulting tornado-like vortices included the formation of a laminar vortex at low swirl ratio, followed by turbulent vortex breakdowns and vortex touchdowns at higher swirl ratios. An extensive study was conducted by Hangan and Kim (2008) to estimate the proper swirl ratio that should be applied to their three-dimensional RANS simulation with Reynolds Stress Model (RSM) turbulence closure, in order to obtain a good match to Doppler radar measurements of a F4 tornado. They introduced a geometric scale and a velocity scale, concluded that the F4 category approximately corresponds to a swirl ratio of 2.0 (as estimated from the tangential and radial velocities at the computational domain boundaries) and, thereby, tentatively related the swirl ratio with the Fujita scale. Table 2 shows a comparison of tornado categorizations from design guides (ASCE 74, 2010; CIGRÉ, 2009) and the Enhanced Fujita Scale for tornadoes (Ramsdell, Jr. and Rishel, 2007).

With respect to F2 tornadoes, adequate field measurements are not yet available, which hinders developments in the laboratory. This is despite the fact that 86% of categorized tornadoes are categorized as F2 or weaker by ASCE 74 (2010). Hamada *et al*. (2010) presented a procedure to estimate the velocity field of a F2 tornado using CFD data (Hangan and Kim, 2008) and the parameters of a F2 tornado defined by the Fujita scale. It should be mentioned that the CFD simulation assumed a smooth ground surface and did not consider either topographical effects or the wind-structure interaction that might occur with transmission line components. Another limitation is the inability of the RSM to generate multiple vortices at high swirl ratios. Subsequently, Natarajan (2011) used Large Eddy Simulation (LES) to capture the multiple vortices phenomena.

Table 2 Tornado classifications

Scale	Fujita Scale				3 - sec gust	Enhanced Fujita Scale	CIGRÉ (2009)			
	Fastest Quarter-mile wind speeds			Cumlative Percentage	(mph)	3 - sec gust (mph)	Gust Wind (2-3 sec gust) (m/sec)	Tornadoes Potential Wind Gust Width	Frequency of Occurance (avergae)	Notes
	Wind Speed	Path length	Path width							
F0	72 (mph) 32.2 (m/sec)	< 1.0 (mile) 1.61 (km)	< 50 (ft) 15.2 (m)	22.9	45 - 78	65 - 85				
F1	73 - 112 (mph) 32.6 - 50 (m/sec)	1.0 - 3.1 (mile) 1.61 - 5.0 (km)	51 - 170 (ft) 15.2 - 52 (m)	57.6	79 - 117	86 - 110				
F2	113 - 157 (mph) 50 - 70.2 (m/sec)	3.2 - 9.9 (mile) 5.0 - 15.9 (km)	171 - 530 (ft) 52 - 162 (m)	86.1	118 - 161	111 - 135	45 - 70	1000 (m)	1/5	Torsional Loading
F3	158 - 206 (mph) 70.6 - 92.1 (m/sec)	10 - 31 (mile) 16 - 50 (km)	531 - 1,670 (ft) 162 - 509 (m)	96.8	162 - 209	136 - 165	70 - 95	400 (m)	1/1000	
F4	207 - 260 (mph) 92.1 - 116.2 (m/sec)	32 - 99 (mile) 51 - 159 (km)	1,671 - 4,750 (ft) 509 - 1,448 (m)	99.5	210 - 261	166 - 200	95 - 120	200 (m)	1/4000	
F5	261 - 318 (mph) 116.2 - 142.2 (m/sec)	100 - 315 (mile) 160 - 507 (km)	4,751 - 6,000 (ft) 1,448 - 1,829	100	262 - 317	> 200	> 120	200 (m)	1/10,000	

3.2 Structural modeling of a transmission line under tornado loading

There are few attempts in the literature to investigate the behaviour of transmission line systems under HIW events. The failure of a self-supported lattice tower under modeled tornado and downburst wind profiles was investigated by Savory *et al*. (2001). The tornado part of the study was based on the wind model developed by Wen (1975). The tower members were modeled using three-dimensional truss elements. The dynamic analysis was done for several cases: (1) tower alone, (2) including the self-weight of the towers and the conductors and (3) without modeling the transmission lines. The failure observed in this study under tornado loads was a shear failure, which is similar to field observations. A limitation of this study is that only the horizontal wind profile corresponding to a F3 tornado was used in the analysis. The vertical component, as well as the turbulence component, of the wind field was neglected. The vertical component of a tornado wind profile has a significant effect on the behaviour of a transmission line ASCE 74 (2010).

The complexity in analyzing transmission line structures under HIW arises from the fact that tornadoes are localized events with relatively narrow path width and complex wind profile. Due to the localized nature of tornadoes, the forces acting on towers and conductors vary based on the location of the event relative to the tower. In fact, some incidents of transmission line failures were attributed to a tornado whose centre was located far from the transmission line (ASCE 74, 2010). The forces in all tower members change significantly with the variation of separation distance between tornado and support tower (R) and incidence angle (θ), as illustrated in Fig. 16. Different types of tower members (e.g. chords or diagonals) have independent critical values of R and θ at which peak internal forces occur in those members.

The behaviour of the conductors is complicated due to its significant nonlinearity. In fact, even though the probability of a transmission line being crossed by a tornado is reportedly high enough to be of concern (Ishac and White, 1994), the American design code ASCE 74 (2010) recommends that the tornado loads on the lines should be neglected because of such complexity. Hamada (2009) discussed the significance of the conductors on the structural response of transmission towers subjected to a tornado. Without considering the turbulence component, it was concluded that the dynamic effects on the towers are minor. This conclusion is due to the high aerodynamic damping of the conductors and the significant difference between the wind loading period (minimum of 13 seconds) and the tower period (about T = 0.5 seconds). Hamada and El Damatty (2011) investigated the variation of the peak forces on tower members with varying tornado location relative to the transmission line system. The dynamic effect associated with the translational motion of the tornado was assessed. In addition, the study assessed the importance of considering the conductors and ground-wires in the analysis of transmission line systems under tornado loading. Altalmas *et al.* (2012) and El Damatty and Hamada (2013) assessed the transmission line failure mechanisms under critical tornado configurations. In addition, predictions were made for the maximum tornado velocity that various lines can withstand before experiencing global failure, for the main type of failure experienced as well as for the path of members susceptible to failure. Hamada and El Damatty (2013) assessed the behaviour of two guyed transmission line structures under the load cases of a F2 tornado wind field, a boundary layer wind, a recommended wind field from an electrical

power company and the recommended tornado loading cases from CIGRÉ. In addition, forces in the transmission tower members were examined for the case of broken wires under F2 tornado wind load. An initial attempt by El Damatty *et al*. (2013), to provide wind loads equivalent to several critical cases of F2 tornado and transmission line structures, is being developed further in ongoing research.

3.3 Proposed Load Cases

Since F2 tornadoes have a cumulative frequency of occurrence of 86% (ASCE, 2010), the literature provided equivalent load cases for an F2 tornado. Parametric studies conducted on six transmission line systems identify the critical R and θ that lead to peak internal forces in transmission towers under tornado load. Accordingly, equivalent loading cases in the X, Y, and Z directions are recommended, where X is perpendicular to the lines, Y is parallel to the lines and Z is the vertical direction. An example of one equivalent critical loading case with R = 100 m and θ = 0°, is shown in Figs. 17 to 20. Figs. 17 and 18 show the applied wind profiles on the transmission tower in the X and Y directions, respectively. Fig. 19 shows the vertical (Z direction) wind profile on the support tower. Fig. 20 shows the transverse wind profile on the transmission lines such as the conductors and the ground-wires.

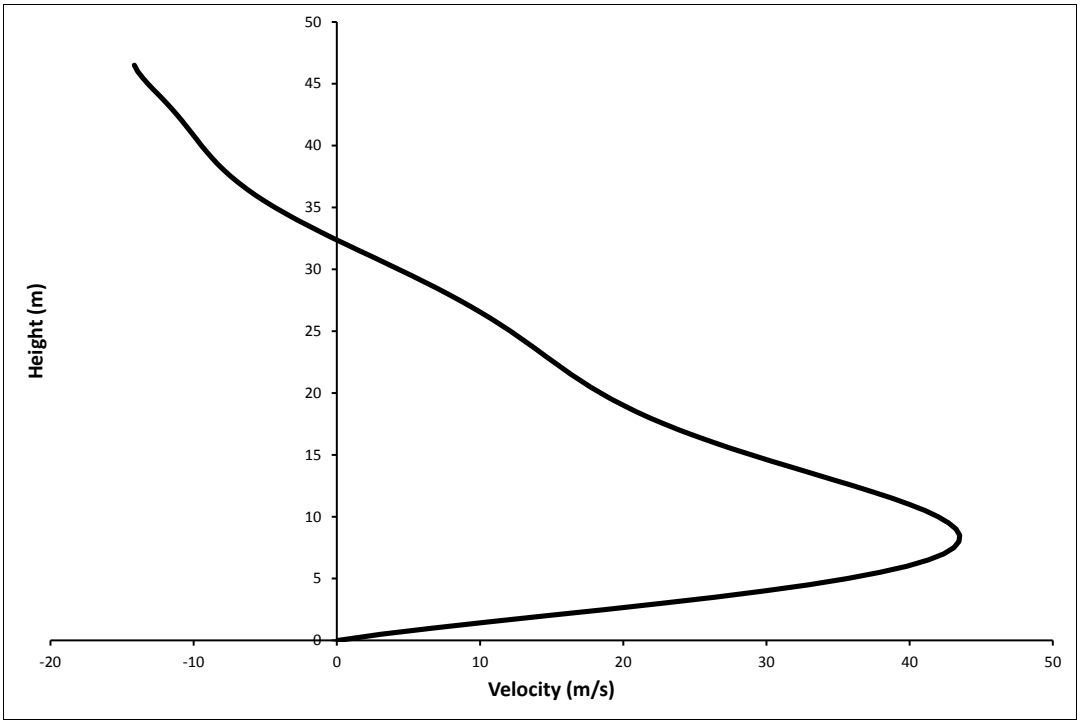

Fig. 17: Velocity profile along transmission tower height – X (transverse) direction

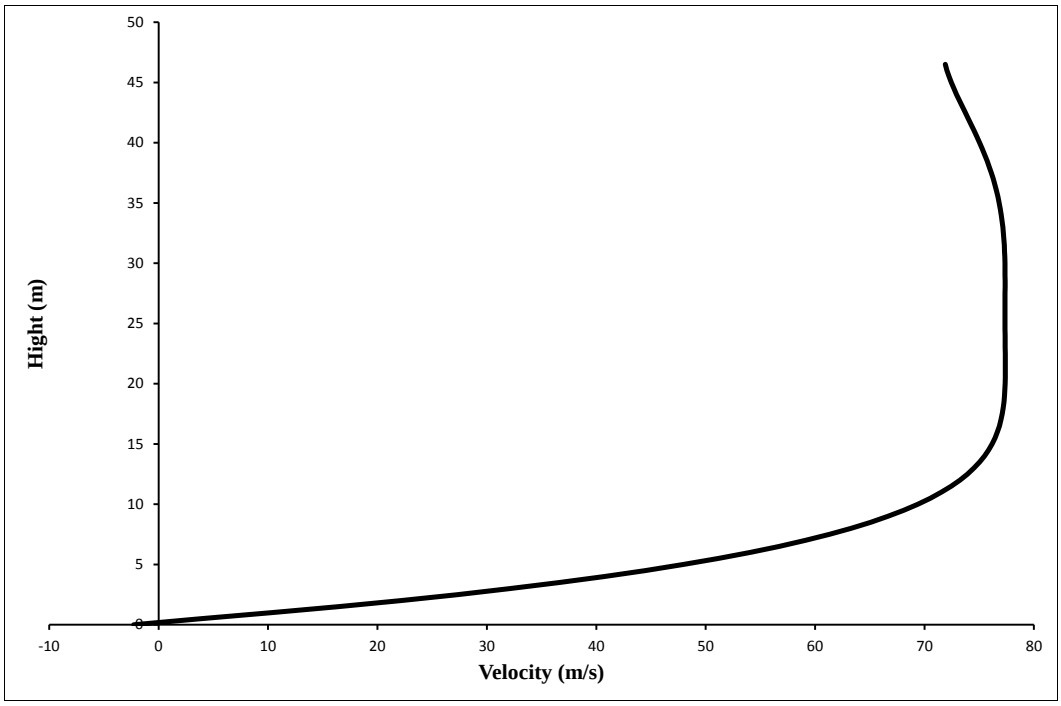

Fig. 18: Velocity profile along transmission tower height – Y (longitudinal) direction

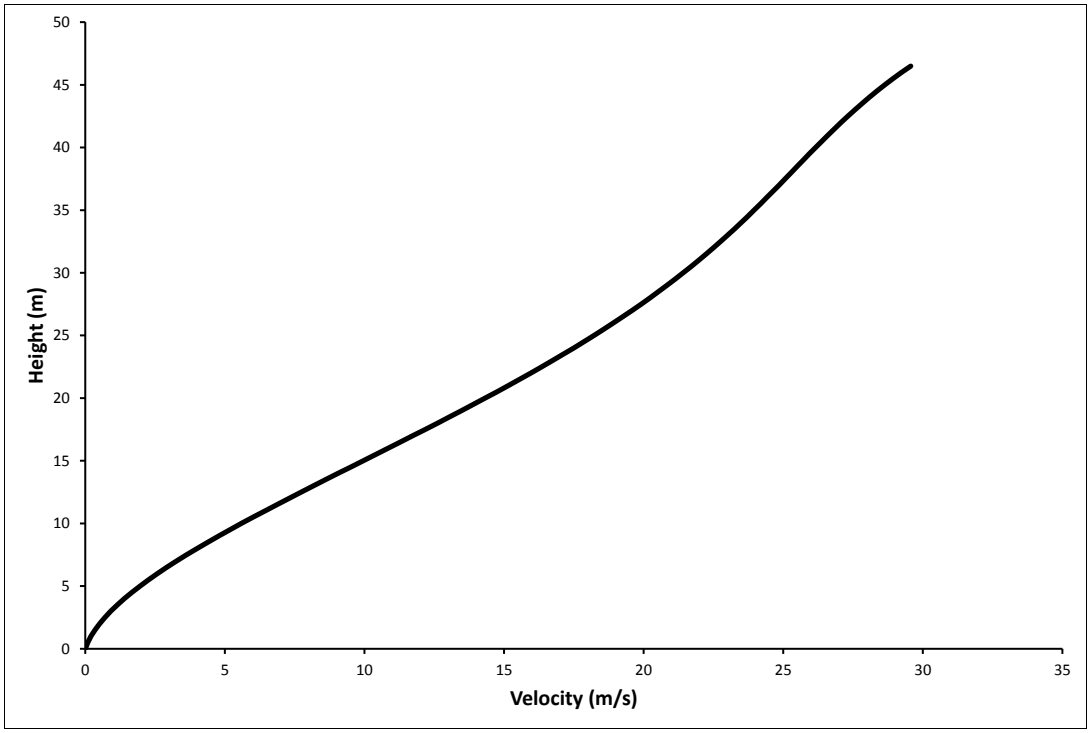

Fig. 19: Velocity profile along transmission tower height – Z (vertical) direction

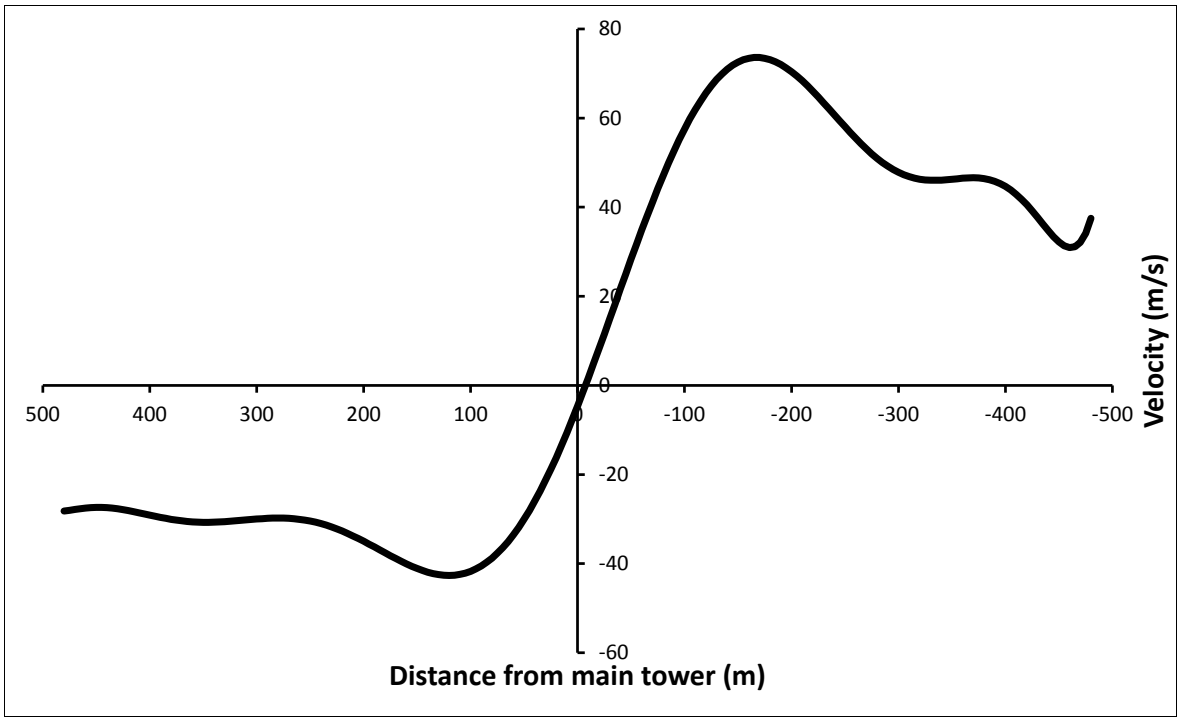

Fig. 20: Transverse velocity profile along the transmission lines

4. SUMMARY AND CONCLUSIONS

This article covers the literature on transmission lines subjected to non-synoptic, high-intensity winds in the form of downbursts and tornadoes. Computational Fluid Dynamics simulations of downbursts and tornadoes have been validated and calibrated with both laboratory experiments and field measurements for damage intensity in the range of F2 to F4 tornado. Downburst field measurements are rare due to the localized nature of this event compared to synoptic wind events. Three different numerical methods have been used to model the downburst wind field, namely the Impinging Jet, Ring Vortex and Cooling Source models. Attempts at modeling the structural response of support tower members, guy wires, the conductor and ground-wire lines in high-intensity winds have identified critical configurations of the wind field and the transmission line system. The size of the downburst or tornado and its location relative to the tower must be considered. In particular, the peak internal forces in all tower members are sensitive to the location of a tornado relative to the transmission tower. Furthermore, it is clear that the vertical profiles of the tangential, radial and vertical velocity components in a tornado wind field significantly differ from the conventional boundary layer wind profile. Some tornado and downburst locations result in unbalanced forces acting on adjacent line spans, a resultant force upon the tower cross-arms in the longitudinal direction of the lines, an out-of-plane bending effect on the cross-arms and, consequently, compression forces in some of the upper chord members. These compression forces might exceed the tension forces that develop in these members due to the self-weight of the conductors and a net compression is not

typically accounted for in structural design based on synoptic wind loads. Dynamic response to a tornado or a downburst tends to be suppressed by large aerodynamic damping of the lines and the long natural period of vibration of the tower. No significant dynamic effects have been found for the lines which have been studied thus far under downburst or tornado wind loading. Gust-induced vibrations are incorporated in most design codes using the Gust Factor (GF) approach. GF is used to scale the forces due to the mean wind speed to account for wind gusts and the structural dynamics. Most codes neglect the resonant response component and account only for effects of the background component of turbulent wind, which is justified for typical towers with natural frequencies exceeding 1 Hz and for conductors with high aerodynamic damping. However, for tall towers and long conductor spans, these conditions might not be valid and, thus, it is recommended that further research is needed to clarify the threshold values of tower frequency and aerodynamic damping below which dynamic effects cannot be neglected.

4.1 Current design codes gaps

Beyond the available simplified treatments, there are limited provisions and significant gaps in structural design codes with respect to non-synoptic winds.

a) Downburst wind load

- In most of the available codes, no clear definition is given for the wind field associated with the downburst events.
    - ✓ Only AS/NZS:7000 (2010) has defined the downburst wind field as a cold air column that falls vertically from a great height and strikes the ground causing a horizontal gust front to radiate outwards from the impact centre.
    - ✓ ASCE 74 (2010) considers the design wind speed to be similar to the F2 tornado range.
- In most of the available codes, no clear definition is given for the velocity profile in the vertical direction. Only AS/NZS:7000 (2010) provides the vertical distribution of the wind speed. Due to the localized nature of downbursts, the velocity profile will depend on the downburst size and its location relative to the tower. Consequently, a number of critical load cases can be identified and should be incorporated in the design codes.
- The effects of terrain and topography on the downburst wind field needs further research before they can be implemented in design codes.
- In all codes, no clear definition is given for the velocity profile along the length of the lines. Depending on the size of the wind event relative to the line span, a nonsymmetrical distribution of the wind pressure over the lines may be a concern which might lead to an unbalanced longitudinal force causing an out-of-plane moment on the tower cross-arms. Such a load case needs to be considered in the design and analysis of support towers.

- Span reduction factor for downburst wind loading is only given in the AS/NZS:7000 (2010). However, the factor provided in this code does not account for the terrain effect or the elevation of the conductor above the ground.
- For flexible tall towers, the dynamic effect should be considered through the gust factor approach proposed by Kwon and Kareem (2009). However, this approach requires further research regarding the turbulence characteristics of the downburst wind field and validation against field measurements.

b) Tornado wind load

- Most codes specialized in designing TLs do not clearly define the velocity profiles along the support structure height and across the conductor spans. These profiles depend on the location of the tornado relative to the transmission tower. As such, a number of critical load cases, reflecting different critical tornado locations, should be identified and incorporated in design codes.
- The effects of terrain and topography on the tornado wind field needs further research before they can be implemented in structural design codes.
- For flexible tall towers, the dynamic effect can be considered through the gust factor approach proposed by Kwon and Kareem (2009). However, this approach requires further research regarding the turbulence characteristics of the tornadic wind field and validation against field measurements.
- For short dynamically insensitive towers, due to the lack of correlation between the fluctuating velocities of the event, a reduction factor may be applied similar to the treatment of synoptic winds. This approach requires further study for its applicability to tornado wind loading.

ACKNOWLEDGEMENT

The authors would like to acknowledge the financial contribution of *The Centre for Energy Advancement through Technological Innovation* (CEATI) to this project. This paper is based on a CEATI report prepared by the authors.

REFERENCES

Aboshosha, H. and El Damatty, A. (2013a), “Downburst induced forces on the conductors of electric transmission lines and the corresponding vulnerability of towers failure”, CSCE 2013 Conference, 29 May – 1 June, Montreal, Canada.

Aboshosha H and El Damatty A. (2013b), “Numerical technique for the reactions of transmission line conductors under high intensity winds”, Wind and Structures, (Accepted for Publication).

Aboshosha H and El Damatty A. (2013c), “Span reduction factor of transmission line conductors under downburst winds”, Proceedings of the 8th Asia-Pacific Conference on Wind Engineering, 10-14 December, Chennai, India.

Altalmas, A., El Damatty, A.A. and Hamada, A. (2012), “Progressive failure of transmission towers under tornado loading”, Proceedings of the Annual Conference of the Canadian Society for Civil Engineering 2012: Leadership in Sustainable

Infrastructure (CSCE 2012), 6-9 June, Canadian Society for Civil Engineering, Edmonton, AB, Canada, 2220-2229.

American Society of Civil Engineers (ASCE) (2010), “Guidelines for electrical transmission line structural loading”, ASCE Manuals and Reports on Engineering Practice, No. 74, New York, NY, USA.

Australian Standard (AS) 1170.2 (2002), “Australian standard for minimum design loads on structures - Part 2: Wind loads”, Standard Australia, North Sydney, Australia.

Australian Standard / New Zealand Standard (AS/NZS) 7000 (2010), “Overhead line design - Detailed procedures”, Standards Australia Limited / Standards New Zealand, North Sydney, Australia.

Baker, D.E. (1981), "Boundary layers in laminar vortex flows", PhD thesis, Purdue University, USA.

Behncke, R.H. and White, H. B. (2006), “Applying Gust Loadings to Your Lines”, Proceedings of the 9th International Conference on Overhead Lines, March, Fort Collins, CO, USA.

Blocken, B., Stathopoulos, T. and Carmeliet, J. (2007), “CFD simulation of the atmospheric boundary layer: wall function problems”, Atmospheric Environment 41(2), 238-252.

Chay, M. T., Albermani, F. and Wilson, R. (2006), “Numerical and analytical simulation of downburst wind loads”, Engineering Structures 28(2), 240-254.

Chay, M. T., Wilson, R. and Albermani, F. (2008), "Gust occurrence in simulated non-stationary winds", Journal of Wind Engineering and Industrial Aerodynamics 96(10), 2161-2172.

Chen, L. and Letchford, C.W. (2004a), "A deterministic–stochastic hybrid model of downbursts and its impact on a cantilevered structure", Engineering Structures 26(5), 619-629.

Chen, L. and Letchford, C.W. (2004b), "Parametric study on the along-wind response of the CAARC building to downbursts in the time domain", Journal of Wind Engineering and Industrial Aerodynamics 92(9), 703-724.

Conseil International des Grands Réseaux Électriques/ International Council on Large Electrical Systems (CIGRÉ) (2001), “Guidelines for field measurement of ice loadings on overhead power line conductors”, CIGRÉ Technical Brochure 179.

Conseil International des Grands Réseaux Électriques/ International Council on Large Electrical Systems (CIGRÉ) (2009), “Overhead line design guidelines for mitigation of severe wind storm damage”, Scientific Committee B2 on Overhead Lines, B2. 06.09.

Darwish, M.M. and El Damatty, A.A. (2011), “Behavior of self supported transmission line towers under stationary downburst loading”, Wind and Structures 14(5), 481-4.

Darwish M., El Damatty A. and Hangan, H. (2010), “Dynamic characteristics of transmission line conductors and behaviour under turbulent downburst loading”, Wind and Structures 13(4), 327-346.

Davenport, A. G. (1967), “Gust loading factors”, ASCE Journal of the Structural Division 93(3), 11–34.

Dempsey, D. and White, H. (1996), “Winds wreak havoc on lines”, Transmission and Distribution World 48(6), 32-37.

Desai, Y.M., Yu, P., Popplewell, N. and Shah, A.H. (1995), “Finite element modelling of transmission line galloping”, Computers and Structures 57(3), 407-420.

Didden, N. and Ho, C.M. (1985), “Unsteady separation in a boundary layer produced by an impinging jet”, Journal of Fluid Mechanics 160, 235–256.

Donaldson, C.D. and Snedeker, R.S. (1971), “A study of free jet impingement, Part 1. Mean properties of free and impinging jets”, Journal of Fluid Mechanics 45, 281–319.

Doswell III, C.A., Brooks, H.E. and Dotzek, N. (2009), “On the implementation of the enhanced Fujita scale in the USA”, Atmospheric Research 93, 554-563.

El Damatty, A. and Aboshosha, H. (2012), “Capacity of electrical transmission towers under downburst loading”, Proceedings of the 1st Australasia and South-East Asia Structural Engineering and Construction Conference, 28 November – 2 December, Perth, Australia, 317-322.

El Damatty, A.A. and Hamada, A. (2013), “Behaviour of guyed transmission line structures under tornado wind loads - Case studies”, Electrical Transmission and Substation Structures 2012: Solutions to Building the Grid of Tomorrow, 4-8 November 2012, ASCE, Columbus, OH, USA, 193-204.

El Damatty, A., Hamada, A. and Elawady, A. (2013), “Development of critical load cases simulating the effect of downbursts and tornadoes on transmission line structures”, Proceedings of the 8th Asia-Pacific Conference on Wind Engineering, 10-14 December, Chennai, India.

Fiedler, B.H. (1994), “The thermodynamic speed limit and its violation in axisymmetric numerical simulations of tornado-like vortices”, Atmosphere-Ocean 32(2), 335-359.

Fiedler, B.H. (1997), “Compressibility and windspeed limits in tornadoes”, Atmosphere-Ocean 35(1), 93-93.

FLUENT Inc. (2005), “FLUENT User’s Guide”, Lebanon, NH, USA.

Fujita, T.T. (1981), “Tornadoes and downbursts in the context of generalized planetary scales", Journal of Atmospheric Sciences 38(8), 1511-1534.

Fujita, T.T. (1985), “The downburst: microburst and macroburst”, SMRP Research Paper 210, University of Chicago, USA.

Fujita, T.T. (1990), "Downbursts: meteorological features and wind field characteristics", Journal of Wind Engineering and Industrial Aerodynamics 36, 75-86.

Fujita, T.T. and Pearson, A.D. (1973), “Results of FPP classification of 1971 and 1972 tornadoes”, Proceedings of the 8th Conference on Severe Local Storms, (abstracts only), USA, 609.

Gant, S.E. (2009), “Reliability issues of LES-related approaches in an industrial context”, Flow, Turbulence and Combustion 84, 325-335.

Gerges, R.R. and El-Damatty, A.A. (2002), “Large displacement analysis of curved beams”, Proceedings of the Canadian Society of Civil Engineering Conference, 3-5 June, Montreal, Canada, ST 100.

Hadžiabdić, M., 2005. LES, RANS and Combined Simulation of Impinging Flows and Heat Transfer Ph.D Thesis. University of Sarajevo 185pp.

Hamada, A., (2009), “Analysis and behaviour of guyed transmission line structure under tornado wind loading”, MESc thesis, The University of Western Ontario, Canada.

Hamada, A., and El Damatty, A.A. (2011), “Behaviour of guyed transmission line structures under tornado wind loading”, Computers and Structures 89(11-12), 986-1003.

Hamada, A., El Damatty, A.A., Hangan, H. and Shehata, A.Y. (2010), "Finite element modelling of transmission line structures under tornado wind loading", Wind and Structures 13(5), 451-469.

Hangan, H. and Kim, J. (2007), "Numerical simulations of impinging jets with application to downbursts", Journal of Wind Engineering and Industrial Aerodynamics 95(4), 279-298.

Hangan, H. and Kim, J. (2008), "Swirl ratio effects on tornado vortices in relation to the Fujita scale", Wind and Structures, 11(4), 291-302.

Hangan, H., Roberts, D., Xu, Z. and Kim, J. (2003), "Downburst simulation. Experimental and numerical challenges", Proceedings of the 11th International Conference on Wind Engineering, 1-5 June, Lubbock, TX, USA.

Harlow, F.H. and Stein, L.R. (1974), "Structural analysis of tornado-like vortices", Journal of Atmospheric Sciences 31(8), 2081-2098.

Hjelmfelt, M.R. (1988), "Structure and life cycle of microburst outflows observed in Colorado", Journal of Applied Meteorology 27, 900–927.

Holmes, J.D. and Oliver, S.E. (2000), "An empirical model of a downburst", Engineering Structures 22, 1167-1172.

Holmes, J.D., Hangan, H.M., Schroeder, J.L., Letchford, C.W. and Orwig, K.D. (2008), "A forensic study of the Lubbock-Reese downdraft of 2002", Wind and Structures 11(2), 137-152.

Irvine, H.M. (1981), "Cable structures", MIT Press, Cambridge, MA, USA.

Ishac, M.F. and White, H.B. (1994), "Effect of tornado loads on transmission lines", Proceedings of the 1994 IEEE Power Engineering Society Transmission and Distribution Conference, 10-15 April 1994, IEEE, Chicago, IL, USA, 521-527.

Ivan, M. (1986), "A ring-vortex downburst model for flight simulations." Journal of Aircraft 23, 232-236.

Kareem, A. (2010), "Bluff body aerodynamics and aeroelasticity: A wind effects perspective", Journal of Wind and Engineering 7(1), 30-74.

Kim, J. and Hangan, H. (2007), "Numerical simulations of impinging jets with application to downbursts", Journal of Wind Engineering and Industrial Aerodynamics 95(4), 279-298.

Kim, J.D., Hangan, H. and Ho, T.C.E. (2007), "Downburst versus boundary layer induced loads for tall buildings", Wind and Structures 10(5), 481-494.

Koziey, B. and Mirza, F. (1994), "Consistent curved beam element", Computers and Structures 51(6), 643–654.

Kwon, D.K. and Kareem, A. (2009), "Gust-front factor: New framework for wind load effects on structures", ASCE Journal of Structural Engineering 135(6), 717-732.

Ladubec, C., El Damatty, A.A. and El Ansary, A.M. (2012), "Effect of geometric nonlinear behaviour of a guyed transmission tower under downburst loading", Proceedings of the International Conference on Vibration, Structural Engineering and Measurement (ICVSEM 2012), 19-21 October 2012, Shanghai, China, Trans Tech Publications, 1240-1249.

Lee, W.-C. and Wurman, J. (2005), "Diagnosed three-dimensional axisymmetric structure of the Mulhall tornado on 3 May 1999", Journal of Atmospheric Sciences 62(7), 2373-93.

Letchford, C.W., Mans, C. and Chay, M.T. (2002), “Thunderstorms—their importance in wind engineering (a case for the next generation wind tunnel)”, Journal of Wind Engineering and Industrial Aerodynamics 90(12), 1415-1433.

Lewellen, D.C., Lewellen, W.S. and Xia, J. (2000), “The influence of a local swirl ratio on tornado intensification near the surface”, Journal of Atmospheric Sciences 57(4), 527-544.

Lewellen, W.S., Lewellen, D.C. and Sykes, R.I. (1997), “Large-eddy simulation of a tornado's interaction with the surface”, Journal of Atmospheric Sciences 54(5), 581-605.

Li, C.Q. (2000), “Stochastic model of severe thunderstorms for transmission line design”, Probabilistic Engineering Mechanics 15(4), 359-364.

Lin, W.E., Savory, E., McIntyre, R.P., Vandelaar, C.S. and King, J.P.C. (2012), “The response of an overhead electrical power transmission line to two types of wind forcing”, Journal of Wind Engineering and Industrial Aerodynamics 100(1), 58–69.

Manitoba Hydro (1999), “Bipole 1 & 2 HVDC Transmission Line Wind Storm Failure on September 5, 1996 – Review of Emergency Response, Restoration and Design of These Lines”, Transmission and Civil Design Department, 98-L1/1-37010-06000, 54 pp.

Mara, T.G., Galsworthy, J.K. and Savory, E. (2010). “Assessment of vertical wind loads on lattice framework with application to thunderstorm winds”, Wind and Structures 13(5), 413-431.

McDonald, J.R., Forbes, G.S. and Marshall, T.P. (2004), “The enhanced Fujita (EF) scale”, Preprints of the 22nd Conference on Severe Local Storms, 3-8 October, Hyannis, MA, USA, American Meteorological Society, CD-ROM B (Vol. 3).

Mason, M.S., Wood, G.S., Fletcher, D.F. (2009), “Numerical simulation of downburst winds”, Journal of Wind Engineering and Industrial Aerodynamics 97(11-12), 523-539.

Mason, M.S., Fletcher, D.F. and Wood, G.S. (2010a), “Numerical simulation of idealized three-dimensional downburst wind fields”, Engineering Structures 32(11), 3558-3570.

Mason, M.S., Wood, G.S. and Fletcher, D.F. (2010b), "Numerical investigation of the influence of topography on simulated downburst wind fields", Journal of Wind Engineering and Industrial Aerodynamics 98(1), 21-33.

McCarthy, P. and Melsness, M. (1996), “Severe weather elements associated with September 5, 1996 hydro tower failures near Grosse Isle, Manitoba, Canada”, Manitoba Environmental Service Centre, Environment Canada.

Menter, F.R. and Egorov, Y. (2010), “The Scale-Adaptive Simulation method for unsteady turbulent flow predictions. Part 1: Theory and model predictions”, Flow, Turbulence and Combustion 85(1), 113-138.

Natarajan, D. (2011), “Numerical simulation of tornado-like vortices”, PhD thesis, The University of Western Ontario, Canada.

Newark, M.J. (1984), “Canadian tornadoes, 1950-1979”, Atmospheric-Ocean 22, 243-253.

Orf, L. G., Kantor, E. and Savory, E. (2012), “Simulation of a downburst-producing thunderstorm using a very high-resolution three-dimensional cloud model”, Journal of Wind Engineering and Industrial Aerodynamics 104-106, 547-557.

Orf, L.G., Oreskovic, C. and Savory, E. (2013), “Circumferential analysis of simulated 3-D downburst-producing thunderstorm outflows”, Proceedings of the 6th European and African Conference on Wind Engineering, Cambridge, UK, July.

Ramsdell, Jr., J.V. and Rishel, J.P. (2007), “Tornado Climatology of the Contiguous United States”, PNNL-15112 Revision 1, Pacific Northwest National Laboratory, Richland, WA, USA. Prepared for U.S. Nuclear Regulatory Commission, NUREG/CR-4461 Revision 2, Washington, DC, USA.

Reynolds, G.W. (1970), “A practical look at tornado forces”, Proceedings of the Conference on Tornado Phenomenology and Related Protective Design Measures, 26-28 April, Madison, WI, USA, Tech Paper No 3, Utah State University, USA, iv, 24 pp.

Reynolds, G.W. (1977), “Wind pressures from ninety combinations of rotational, translational, and convergent velocities for each of eight vortex positions”, Proceedings of the Symposium on Tornadoes, Assessment of Knowledge and Implications for Man, 22-24 June 1976, Lubbock, TX, USA, edited by R.F. Abbey and K.C. Mehta, sponsored by Institute for Disaster Research at Texas Tech University, 449-461.

Rotunno, R. (1977), “Numerical simulation of a laboratory vortex tornado theory”, Journal of Atmospheric Sciences 34(12), 1942-1956.

Rotunno, R. (1979), “A study in tornado-like vortex dynamics”, Journal of Atmospheric Sciences 36(1), 140-155.

Rotunno, R. (1984), “An investigation of a three-dimensional asymmetric vortex”, Journal of Atmospheric Sciences 41(2), 283-298.

Sarkar, P., Haan, F., Gallus Jr., W., Le, K. and Wurman, J. (2005), “Velocity measurements in a laboratory tornado simulator and their comparison with numerical and full-scale data”, Proceedings of the 37th Joint Meeting Panel on Wind and Seismic Effects, 16-21 May, Tsukuba, Japan.

Savory, E., Parke, G.A.R., Zeinoddini, M., Toy, N., and Disney, P. (2001), “Modelling of tornado and microburst-induced wind loading and failure of a lattice transmission tower”, Engineering Structures 23(4), 365-375.

Selvam, R.P. and Holmes, J.D. (1992), “Numerical simulation of thunderstorm downdrafts”, Journal of Wind Engineering and Industrial Aerodynamics 41–44, 2817–2825.

Sengupta, A., Sarkar, P.P., 2008. Experimental measurement and numerical simulation of an impinging jet with application to thunderstorm microburst winds. Journal of Wind Engineering and Industrial Aerodynamics 96, 345–365.

Shehata, A.Y. and El Damatty, A.A. (2007), “Behaviour of guyed transmission line structures under downburst wind loading”, Wind and Structures 10(3), 249-268.

Shehata, A.Y. and El Damatty, A.A. (2008), “Failure analysis of a transmission tower during a microburst”, Wind and Structures 11(3), 193-208.

Shehata, A.Y., El Damatty, A.A. and Savory, E. (2005), “Finite element modeling of transmission line under downburst wind loading”, Finite Elements in Analysis and Design 42(1), 71-89.

Shehata, A. Y., Nassef, A.O. and El Damatty, A.A. (2008), "A coupled finite element-optimization technique to determine critical microburst parameters for transmission towers", Finite Elements in Analysis and Design 45(1), 1-12.

Trapp, R.J. and Fiedler, B.H. (1995), "Tornado-like vortexgenesis in a simplified numerical model", Journal of Atmospheric Sciences 52(21), 3757-3778.

Twisdale, L.A. (1982), "Regional tornado data base and error analysis", Preprints of the 12th Conference on Severe Local Storms, 11-15 January, San Antonio, TX, USA, American Meteorological Society, 45–50.

Vermeire, B.C., Orf, L.G. and Savory, E. (2011a), "Improved modelling of downburst outflows for wind engineering applications using a cooling source approach", Journal of Wind Engineering and Industrial Aerodynamics 99(8), 801-814.

Vermeire, B.C., Orf, L.G. and Savory, E. (2011b), "A parametric study of downburst line near-surface outflows", Journal of Wind Engineering and Industrial Aerodynamics 99(4), 226-238.

Vicroy, D. D. (1992), "Assessment of microburst models for downdraft estimation", Journal of Aircraft 29, 1043-1048.

Wang, X., Lou, W., Li, H. and Chen, Y. (2009), "Wind-induced dynamic response of high-rise transmission tower under downburst wind load", Journal of Zhejiang University 43(8), 1520-1525.

Ward, N.B. (1972), "The exploration of certain features of tornado dynamics using a laboratory model", Journal of Atmospheric Sciences 29, 1194-1204.

Wei, P., Bingnan, S. and Jinchun T. (1999), "A catenary element for the analysis of cable structures", Applied Mathematics and Mechanics (English Edition) 20(5), 0253-4827.

Wen, Y.-K. (1975), "Dynamic tornadic wind loads on tall buildings", ASCE Journal of the Structural Division 101(1), 169-185.

Wieringa, J. 1992. Updating the Davenport roughness classification. Journal of Wind Engineering and Industrial Aerodynamics 41-44, 357-368.

Winkelman, P.F. (1959), "Sag-tension computations and field measurements of Bonneville Power Administration", AIEE Paper 59-900.

Wolfson, M. M., DiStefano, J.T. and Fujita, T.T. (1985), "Low-altitude wind shear characteristics in the Memphis, TN area", Preprints of the 14th Conference on Severe Local Storms, October 29 – November 1, Indianapolis, IN, USA, American Meteorological Society, 322–327.

Wood, G. S., Kwok, K. C. S., Motteram, N. A. and Fletcher, D. F. (2001), "Physical and numerical modelling of thunderstorm downbursts", Journal of Wind Engineering and Industrial Aerodynamics 89, 535-552.

Wurman, J. (1998), "Preliminary results from the ROTATE-98 tornado study", Proceedings of the 19th Conference on Severe Local Storms, 14-18 September, Minneapolis, MN, USA, American Meteorological Society, 120-123.

Yu, P., Wong, P. and Kaempffer, F. (1995), "Tension of conductor under concentrated loads", Journal of Applied Mechanics – Transactions of the American Society of Mechanical Engineers 62(3), 802-809.

Zhou, Y., and Kareem, A. (2001). "Gust loading factor: New model." J. Struct. Eng., 127(2), 168–175.

Zhu, S. and Etkin, B. (1985), "Model of the wind field in a downburst", Journal of Aircraft 22, 595-601.